EVS30 Symposium
Stuttgart, Germany, October 9 – 11, 2017

Li-ion Battery Lifetime Model Influence on the Economic Assessment of a Hybrid Electric Bus Operation

E. Martinez-Laserna*, V.I. Herrera, I. Gandiaga, A. Milo, E. Sarasketa-Zabala, H. Gaztañaga

*IK4-IKERLAN, Pº J. M. Arizmendiarrieta 2, Arrasate, 20500, Spain, *emartinez@ikerlan.es*

Abstract

The present paper is focused on the evaluation of the economic influence of the battery lifetime model over the optimal sizing and energy management strategy of a dual energy storage system (ESS), composed of Lithium-ion batteries and supercapacitors. The operation of a Hybrid Bus is taken as a case study to evaluate the effects of battery lifetime models' accuracy on ESS sizing and operation in a heavy-duty application. For this purpose, two different lifetime models (a Wöhler-curve based model and a semi-empirical model) were applied in the multi-objective optimisation of a hybrid electric urban bus. Differences up to *c.a.* 8% on the daily operation costs and *c.a.* 25% on the dual ESS costs were estimated depending on the lifetime model that was considered for the optimisation.

Keywords: Li-ion Battery, Hybrid Energy Storage System, Lifetime model, Multi-objective optimisation.

1 Introduction

The development of new electrochemical energy storage technologies and the growing maturity of lithium-ion (Li-ion) batteries are promoting the penetration of advanced electro-mobility solutions. In the urban context, one of the most promising alternatives to reduce emissions is the use of hybrid electric buses (HEB), considered a more viable alternative than full-electric buses in the medium term [1].

The implementation of battery-based energy storage systems (ESS) entails inherent challenges, since the reduction of fuel consumption is related to a higher use of the batteries. This leads to a great number of battery charge/discharge cycles and thus its potential early degradation [2], which might imply multiple replacements to cover the lifetime of a heavy-duty application, as it is the case of urban buses. Therefore, extending battery lifetime results crucial to make electric or hybrid buses a cost-competitive alternative to conventional buses [3]. To solve this issue, the use of a dual ESS, composed of batteries and supercapacitors, is investigated in this paper.

In this context, the lifetime model of the battery becomes an important tool to evaluate their degradation behaviour during vehicle operation, as their lifetime is reported to be typically shorter than that of supercapacitors [4]. The proper assessment of battery lifetime may even affect the design and definition of business models either for vehicle manufacturers or vehicle operators, conditioning how certain economic targets could be achieved [1]. Nevertheless, most publications in literature rarely emphasize on lifetime modelling when describing the sizing and operation of a dual ESS.

The aim of this paper is to analyse the techno-economic influence of the battery lifetime model on the sizing and operation of a hybrid ESS. Two different battery lifetime models were considered for the targeted multi-objective (MO) optimization: i) a Wöhler-curve based lifetime model (simple and cost-efficient but less accurate) and ii) a semi-empirical lifetime model (costly and time-consuming, but accurate) [5]. Results obtained in the optimizations carried out with each lifetime model are compared in

economic terms, and the ageing behaviour estimated with each model is analysed to approach how the dual ESS would perform on the real application.

2 Scenario Overview

The scenario analysed in this paper is based on a Series Hybrid Electric Bus (SHEB) for urban operation. Fig. 1 depicts the powertrain configuration of the SHEB including a dual ESS [6]. The main propulsion element is the electric motor (EM) powered from the DC bus and mechanically connected to the vehicle transmission (T). The EM operates as generator during regenerative braking phase. The SHEB includes a dual ESS composed of: Li-ion battery that provides high energy density, as the main energy storage unit, and a supercapacitor system with high power density, which is conceived to absorb or inject power peaks during the regenerative braking or acceleration events, respectively. Among the different possible dual ESS connection topologies [7], a fully active or parallel connection topology was selected to allow decoupling the operation of batteries and supercapacitors, in order to maximise the functionalities of each energy storage technology. The genset considered includes an Internal Combustion engine (ICE) and an electric generator (EG) set.

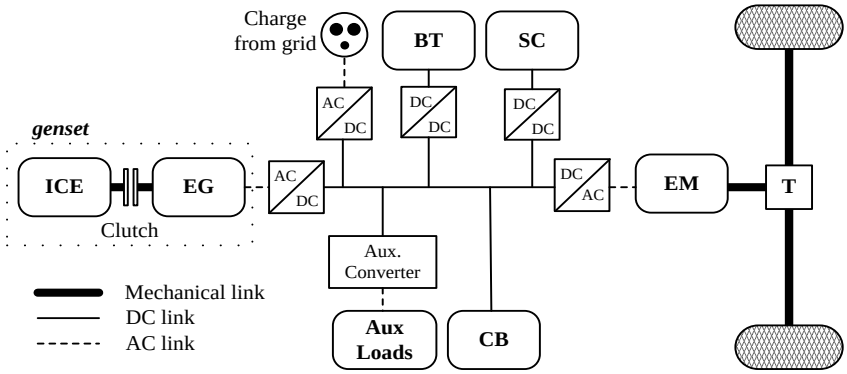

Fig. 1. Series Hybrid Electric Bus powertrain configuration.

The route profile considered includes several stops (which were considered as zero emission zones), a maximum speed of 50 km/h, a travelling distance or around 27 km (round trip), also including a full-electric operation zone with a driving section of around 2.4 km. Thus, the considered SHEB is intended to operate both on hybrid mode (powered by the genset and the dual ESS) and in full-electric mode (only propelled by the dual ESS). The speed profile depicted in Fig. 2 was repeated several times to complete a daily profile of 16 hours of operation.

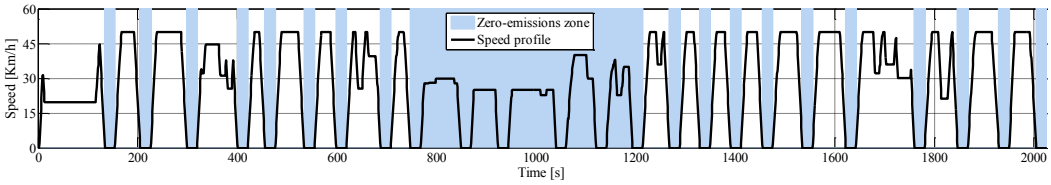

Fig. 2. Speed profile for HEB operation.

The simulation model was developed in Matlab/Simulink. The powertrain was modelled following a backward or effect-cause approach [6] Optimal Energy Management of a Hybrid Electric Bus with a Battery-Supercapacitor Storage System using Genetic Algorithms Optimal Energy Management of a Hybrid Electric Bus with a Battery-Supercapacitor Storage System using Genetic Algorithms. It calculates the power consumed by the bus at each discrete step following a predefined speed profile by going upstream through the vehicle components [6].

3 Modelling of the Onboard Dual ESS

3.1 Electrical Modelling

The dual ESS considered is composed of a SC pack and Li-ion BT pack connected on a parallel topology, as described in the previous section. The electrical modelling was simplified to limit the computational

cost, assuming that the error obtained on the estimated voltage response of the SC and BT would not have a significant impact over the optimal sizing of the dual ESS.

A supercapacitor model consisting of a 3000 F electric double-layer capacitor C_{SCcell} [F] in series with a resistance $R_{int-SCcell}$ [Ω] was implemented, as described in Fig. 3. Assuming that a string contains S_{SC} supercapacitor cells in series and the SC pack groups B_{SC} strings in parallel, the equations describing the electrical behaviour of each SC pack were implemented as follows:

$$C_{SC} = B_{SC} \cdot C_{SCcell} / S_{SC} \ [F] \quad (1)$$

$$R_{SC} = S_{SC} \cdot R_{int\_SCcell} / B_{SC} \ [\Omega] \quad (2)$$

being C_{SC} [F] and R_{SC} [ohm] the equivalent capacitance and equivalent internal resistance for the SC pack, respectively.

Regarding the Li-ion BT, a 2.3 Ah LFP-based Li-ion battery reference was considered. Similarly to the case of the SC pack, each Li-ion battery was modelled by means of the open circuit voltage (OCV) of the cell (V_{OC_BTcell} [V]) in series with a resistor (R_{int_BTcell} [ohm]), which models its DC internal resistance, as described in Fig. 3. Assuming that a string contains S_{BT} battery cells in series and the BT pack groups B_{BT} strings in parallel, the equations describing the electrical behaviour of each BT pack were implemented as follows:

$$U_{BT} = V_{OC\_BTcell} \cdot S_{BT} \ [V] \quad (3)$$

$$R_{BT} = S_{BT} \cdot R_{int\_BTcell} / B_{BT} \ [\Omega] \quad (4)$$

being U_{BT} $[V]$ and R_{BT} $[ohm]$ the voltage and equivalent internal resistance for the BT pack, respectively.

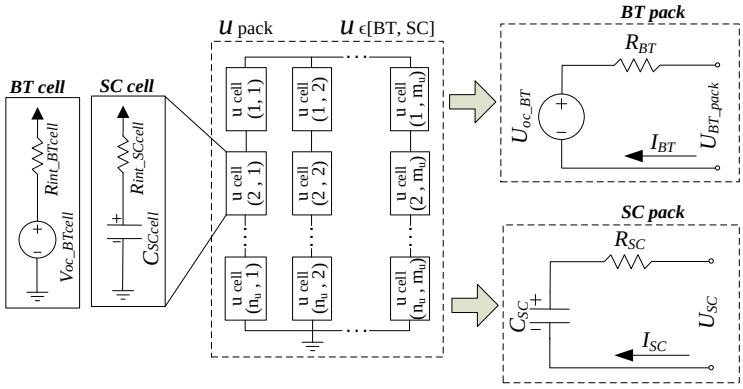

Fig. 3. Battery and Supercapacitor pack configuration.

Table I summarises the main parameters of the battery and supercapacitor references considered in this scenario. On the one hand, the maximum C-rate for charging and discharging the batteries was limited to 3.5C to maintain the reliability of the lifetime model considered (described in the next section), and extend battery lifetime[8].

TABLE I:
ELECTRICAL PARAMETERS OF BT AND SC BASE CELLS [9].

BT (LFP 2.3Ah 26650-type)		SC (BCAP3000)	
Nominal voltage	3.3 V	Nominal voltage	2.7 V
Nominal capacity	2.3 Ah	Nominal capacitance	3000 F
DC internal resistance	$R_{int}(SOC_{BT})$ ohm	DC internal resistance	0.29 $m$ohm
Max C-rate disch./ch.	3.5/3.5	-	-
Gravimetric Energy Density	108 Wh/kg	Gravimetric Energy Density	6.0 Wh/kg
# cells in series (pack)	182	# cells in series (pack)	144
DC/DC converter rating	50 kW	DC/DC converter rating	150 kW

3.2 Lifetime Modelling

With respect to the ageing performance of the supercapacitors, it was considered that these devices can typically withstand a significant amount of cycles, comparatively larger than Li-ion batteries. Therefore, a constant value of 10^6 cycles and a maximum lifetime of 10 years were implemented as the upper limit for SC lifetime. On the contrary, the lifetime estimation of the Li-ion batteries was one of the core elements of the present study. Two different battery lifetime models were considered to evaluate their impact upon the ESS sizing and the determination of the optimal operation constraints: i) a Wöhler curve based lifetime model and ii) a semi-empirical lifetime model. These two different approaches represent different levels of complexity and experimental labour costs, but also are unequally accurate for prediction BT lifetime on real operation condition.

3.2.1 Wöhler Curve Based Lifetime Model:

The use of Wöhler curve based ageing models has been typically considered in literature, especially for sizing purposes or for economic analyses in applications where a battery based ESS is integrated.

The idea behind this modelling approach consists of mathematically expressing the number of events i that can occur during the lifetime of a battery until it reaches its End-of-Life (EOL), as indicated in Eq. (5). In this case, i represents a certain Depth of Discharge (DoD) and the model evaluates the effect of the DoD upon the degradation of the battery using a *Rainflow* cycle counting algorithm [10], [11]. LL_i represents the lifetime decrease caused by the occurrence of a certain number of i events (*i.e.* the number of charge-discharge full cycles at a certain DoD).

$$LL_i = \frac{NE_i}{NE_i^{max}} \tag{5}$$

where NE_i^{max} is the maximum number of events i that the battery can withstand and NE_i the number of events accounted. Thereby, LL_i represents the lifetime lost as consequence of the occurrence of a certain number of i events – *i.e.* as a consequence of a number of charge-discharge cycles at a certain DoD –. Similarly, for the whole range of DoD (from 0 to 100%), the total loss of lifetime is expressed according to equation (6):

$$LL = \sum_i LL_i \tag{6}$$

Accordingly, when the lifetime lost LL equals 1, it is considered that the cell has reached the EOL.

This method allows evaluating the corresponding loss of lifetime for a certain battery State of Charge (SOC) profile, from which the number of events at each DoD range can be defined. Then, considering the duration of SOC profile introduced, the total lifetime can be calculated as the inversion of LL, typically defined in years (for a one-year SOC profile):

$$Lifetime = \frac{1}{LL} \tag{7}$$

The maximum number of events NE_i^{max} at each DoD was deduced from the Wöhler curve of the batteries considered. In this case, for the considered LFP-based cell, the Wöhler curve obtained from experimental testing described in Ref. [12] was implemented.

3.2.2 Semi-Empirical Lifetime Model:

A thorough semi-empirical lifetime model comprising both cycling and calendar ageing was implemented in the study. Such ageing model allowed more accurately evaluating the impact of the lifetime model upon the dual ESS sizing [12]. The implemented semi-empirical battery lifetime model evaluates the capacity fade experienced over the time by superimposing the effect of calendar and cycle operation.

The capacity loss due to calendar life $Q_{loss_{cal}}$ [%] was calculated as described in Ref. [13], according to equation (8):

$$Q_{loss_{cal}}[\%] = \alpha_1 \cdot e^{\beta_1 \cdot T^{-1}} \cdot \alpha_2 \cdot e^{\beta_2 \cdot SOC} \cdot t^{0.5} \quad (8)$$

where T [K] and SOC [%] are the ambient temperature and the state of charge at which the cell is stored, t is time elapsed on storage and $\alpha_1, \alpha_2, \beta_1, \beta_2$ are fitting coefficients.

The capacity loss due to cycling $Q_{loss\ cyc}$ [%], was calculated as described in Ref. [8], according to equations (9,10). In this case, the effect of the C-rate was neglected (as it was limited to 3.5C) and only the effects of the DoD and the Ampere hour throughput were considered. Details about cycle ageing behaviour and specific modelling issues can be found in Refs. [5], [8].

$$Q_{loss_{cyc}}(10\% \leq DOD \leq 50\%) = (\gamma_1 \cdot DOD^2 + \gamma_2 \cdot DOD + \gamma_3) \cdot k \cdot Ah^{0.87} \quad (9)$$

$$Q_{loss_{cyc}}(10\% > DOD > 50\%) = \left(\alpha_3 \cdot e^{\beta_3 \cdot DOD} \cdot \alpha_4 \cdot e^{\beta_4 \cdot DOD}\right) \cdot k \cdot Ah^{0.65} \quad (10)$$

where $Q_{loss\ cyc}$ [%] is the equivalent capacity fade caused by cycling; DOD [%] represents the DoD at which the cycles are performed, and Ah the Ampere hours-throughput during the considered cycling period. Additionally, $\gamma_1, \gamma_2, \gamma_3, \alpha_3, \alpha_4, \beta_3$ and β_4 are constant fitting coefficients and k represents the acceleration factor of the caused by static cycling ageing tests [8].

Finally, the resultant total capacity loss Q_{loss} [%] is calculated as the superposition of the capacity loss caused by calendar life $Q_{loss_{cal}}$ and by cycle life ageing $Q_{loss_{cyc}}$ [5] as shown in equation (11).

$$Q_{loss}[\%] = Q_{loss_{cal}} + Q_{loss_{cyc}} \quad (11)$$

The precision of this model has been thoroughly validated under different ageing conditions based on the methodology deeply described in [5], [12]. For all the cases considered in validation, the RMSE prediction error calculated for the semi-empirical ageing model was below 1.4%.

4 Rule-based Energy Management Strategy

In order to operate the vehicle under the scenarios of hybrid and full-electric performance, and also considering the proposed dual ESS, different operation modes were defined[14]. The performance of the Rule-Based Energy Management Strategy (RB-EMS) thus depends on the instantaneous *driving mode.*

4.1 Hybrid driving mode

In this operation mode both the genset and the dual ESS operate together. As depicted in Fig. 4, the performance of the *hybrid driving mode* depends on the State of Charge of the battery (SOC_{BT}) with two defined control levels (SOC_{u_ctrl} and SOC_{l_ctrl}) in order to select the *energy mode* for the SHEB operation. Thus, within *hybrid driving mode* the following energy modes were defined: i) Depleting mode (DM), ii) Sustaining mode (SM) and iii) Charging mode (CM).

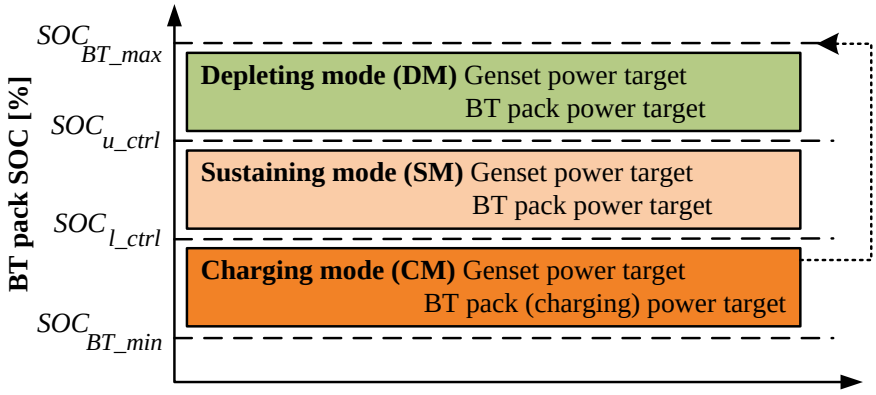

Fig. 4. EMS (energy modes) in hybrid driving mode.

In the first two modes both genset and BT pack supply vehicle energy demands. Fig. 5 depicts the proposed strategy to split the power demand among the genset, BT and SC pack, mathematically described according to equations (12)-(14):

$$P_{BT\_dch} = \left(V_{nom\_BTcell} \cdot S_{BT}\right)\left(I_{1C\_BTcell} \cdot C_{rate} \cdot B_{BT}\right) \cdot p_{dch}/10^3 \quad (12)$$

$$P_{BT\_dch} = \left(V_{nom\_BTcell} \cdot S_{BT}\right)\left(I_{1C\_BTcell} \cdot C_{rate} \cdot B_{BT}\right) \cdot p_{ch}/10^3 \quad (13)$$

$$P_{genset}\,(k) = P_{DEM}\,(k) + P_{BT\_ch} \quad (14)$$

being:

- $P_{genset}\,(k)\ [kW]$ the genset power target.
- P_{BT_dch} [kW] the BT power target during discharge.
- $P_{BT\_ch}\ [kW]$ the BT power target during charge.
- $V_{nom\_BTcell}\ [V]$ the nominal voltage of the BT cell.
- $I_{1C\_BTcell}\ [A]$ the nominal current of the BT cell.
- C_{rate} the C-rate limitation for the BT operation.
- p_{dch} the ratio for BT pack discharging ($p_{dch} \in [0 - 1]$) with different values for DM, SM and AM.
- p_{ch} the ratio for charging the BT pack ($p_{ch} \in [0 - 1]$).
- $E_{CB}\ [kWh]$ the energy dissipated in crowbar.
- $P_{SC\_max\_ch}\ [kW]$ the maximum allowable power target for charging the SC pack (maximum power of the DC/DC).

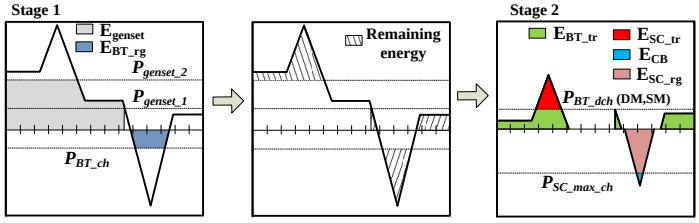

(a) Depleting and Sustaining mode

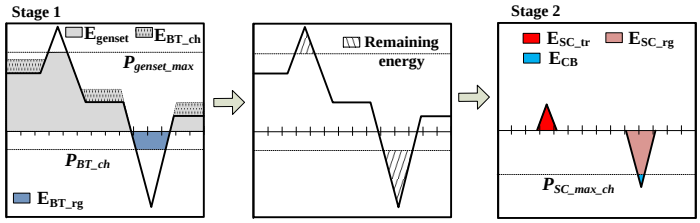

(b) Charging mode

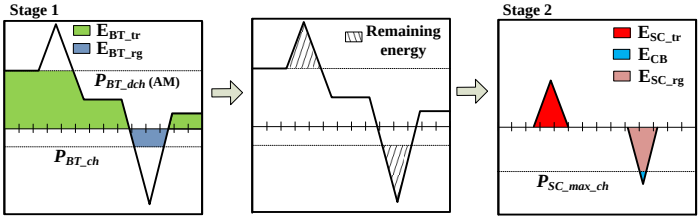

(c) Full-electric driving mode

Fig. 5. Power split strategy.

4.2 Full-electric driving mode

In this mode, Fig. 5 (c), only the dual ESS operates to propel the vehicle while the genset is turned-off. During traction phase ($P_{DEM}\,(k) \geq 0$), the power target $P_{BT\_dch}\ [kW]$ (equation (12)) was configured at the maximum optimal power target for discharging ($p_{dch} = p_{dch\_AM}$). The remaining energy would then be supplied by SC pack.

In regenerative braking phase ($P_{DEM}\,(k) < 0$) the same power targets ($P_{BT\_ch}\ [kW]$, $P_{SC\_max\_ch}\ [kW]$), as in *hybrid driving mode*, were applied.

5 Multi-objective optimization problem

To apply the MO optimization on the scenario proposed in this paper, the fitness function that quantifies the score of each evaluated solution pursues finding the minimum operation costs for the SHEB, as described in equation (15):

$$\min_{X \in \Omega} C_T(X) = [BT_{Tcost}(X), SC_{Tcost}(X), Fuel_{Tcost}(X)] \tag{15}$$

where C_T $[€/day]$ represents the total operation cost of the SHEB. $BT_{Tcost}(X)$, $SC_{Tcost}(X)$ and $Fuel_{Tcost}$ are represented by economic models to estimate the operation cost of the BT, SC pack and genset, respectively. X is the vector containing the design variables in the proposed optimisation, equation (16), subject to the constraints of the space of feasible solutions described in equation (17).

$$X = [SOC_{u\_ctrl},\ SOC_{l\_ctrl},\ P_{genset\_1},\ P_{genset\_2},\ p_{dch\_DM},\ p_{dch\_SM},\ p_{dch\_AM},\ p_{ch\_CM},\ B_{BT},\ B_{SC}\ ] \tag{16}$$

$$\Omega = \begin{cases} 50 \le SOC_{u_{ctrl}} \le 95\ [\%] \Rightarrow SOC_{u_{ctrl}} \in \mathbb{Z} \\ 40 \le SOC_{l_{ctrl}} \le 85\ [\%] \Rightarrow SOC_{l_{ctrl}} \in \mathbb{Z} \\ 30 \le P_{genset_1} \le 80\ [kW] \Rightarrow P_{genset_1} \in \mathbb{Z} \\ 80 \le P_{genset_2} \le 155\ [kW] \Rightarrow P_{genset_2} \in \mathbb{Z} \\ 0 \le p_{dch}(DM, SM, AM), p_{ch}(CM) \le 1 \Rightarrow p_{dch}, p_{ch} \in \mathbb{R} \\ 1 \le B_{BT} \le 25\ [branches] \Rightarrow B_{BT} \in \mathbb{Z} \\ 1 \le B_{SC} \le 10\ [branches] \Rightarrow B_{SC} \in \mathbb{Z} \end{cases} \tag{17}$$

In this scenario the variables S_{BT} and S_{SC} were assumed as constant in order to reach a battery pack voltage of 600 V and a supercapacitor voltage of 390 V. Thus, the dual ESS sizing optimization will only consider the variation of energy capacity (number of branches: B_{SC}, B_{BT}). The MO problem is solved by means of genetic algorithms (GA). The iterative process carried out by the GA is described in detail in [15].

5.1 Operation cost of the dual ESS

The total operation cost of the dual ESS was defined according to equation (18) [9]. As it can be observed, the term u refers to either the battery or the supercapacitor packs. Thus, the cost components corresponding to battery and supercapacitor pack costs in equation (15) are calculated equally according to the following equations.

$$u_{Tcost} = \left(u_{M_y} + u_{Ca_y} + u_{Re_y}\right)/360\ u\ \epsilon\ [BT, SC] \tag{18}$$

being u_{M_y} $[€/year]$ the annualised maintenance cost of the u pack. The annualised capital cost for the u pack u_{Ca_y} $[€/year]$ was defined as follows:

$$u_{Ca_y} = \left(C_{kW_{dcdc}} \cdot P_{dcdc_u} + C_{kWh_u} \cdot Ca_u\right) \cdot \frac{I \cdot (1+I)^T}{(1+I)^T - 1} \tag{19}$$

being C_{kW_dcdc} $[€/kW]$ the referential cost of the DC/DC converter; P_{dcdc_u} $[kW]$ the power rate of the DC/DC converter; C_{kWh_u} $[€/kWh]$ the referential cost of the u technology; Ca_u $[kWh]$ the sizing of the u pack; I [%] and T $[years]$ the banking interest rate and the lifetime of the whole system (SHEB).

The annualised replacement cost (cycling cost) of the u pack, u_{Re_y} $[€/year]$, were defined as follows:

$$u_{Re_y} = \sum_{i=1}^{ceil\,(T/Life_u - 1)} \left[C_{kWh_u} \cdot Ca_u \cdot \frac{I \cdot (1+I)^T}{(1+I)^T + 1}\right] \cdot \left[(1+I)^{-i \cdot Life_u}\right] \tag{20}$$

where $ceil(x)$ rounds its argument x to the higher integer value; $Life_u$ $[years]$ is the lifetime estimation for the u pack, provided by the corresponding lifetime model (as described in section 3.2).

6 Results and discussion

The optimisation of the operation constraints and the sizing of the dual ESS was performed considering the two different battery lifetime models described in section 3.2. In the two cases, all the remaining elements of the modelled SHEB were unaltered, including the EMS, route, dual ESS electrical models and the lifetime model employed to estimate the lifespan of the supercapacitor pack.

Fig. 6 shows the 3 solutions selected from the Pareto front obtained in the optimisation with the Wöhler curve based (a) and the semi-empirical (b) lifetime models. The solution #1 was selected as the most suitable solution for each of the two cases. TABLE II summarises the optimal set of values for the design variables assigned for the optimisations performed with each lifetime model.

TABLE II: Optimal solution selected for the two optimisation cases.

	Wöhler-based optimisation	Semi-empirical based optimisation
SOC_{u_ctrl} [%]	66	93
SOC_{l_ctrl} [%]	39	44
P_{genset_1} [kW]	53	63
P_{genset_2} [kW]	83	124
p_{dch_DM} [kW]	78	71
p_{dch_SM} [kW]	81	25
p_{dch_AM} [kW]	21	30
p_{ch_CM} [kW]	81	77
B_{BT} [-]	12	10
B_{SC} [-]	2	2

In the case of the optimal solution calculated with the Wöhler curve based lifetime model, the dual ESS would be composed of a battery pack of 16.56 kWh (182S12P) and a supercapacitor pack of 0.86 kWh (144S2P). Considering the optimal values for the operation constraints calculated in that particular optimal case, the operating costs of the SHEB would be *c.a.* 170 €/day, being the daily costs of the batteries and supercapacitors 37.2 and 30.6 €/day, respectively. On the contrary, for the optimal solution calculated with the semi-empirical lifetime model, the selected sizing for the dual ESS would be composed of a battery pack of 13.80 kWh (182S10P) and a supercapacitor pack of 0.86 kWh (144S2P). In that case, the operating costs of the SHEB would be *c.a.* 183 €/day, being the daily costs of the batteries and supercapacitors 19.8 and 30.9 €/day, respectively.

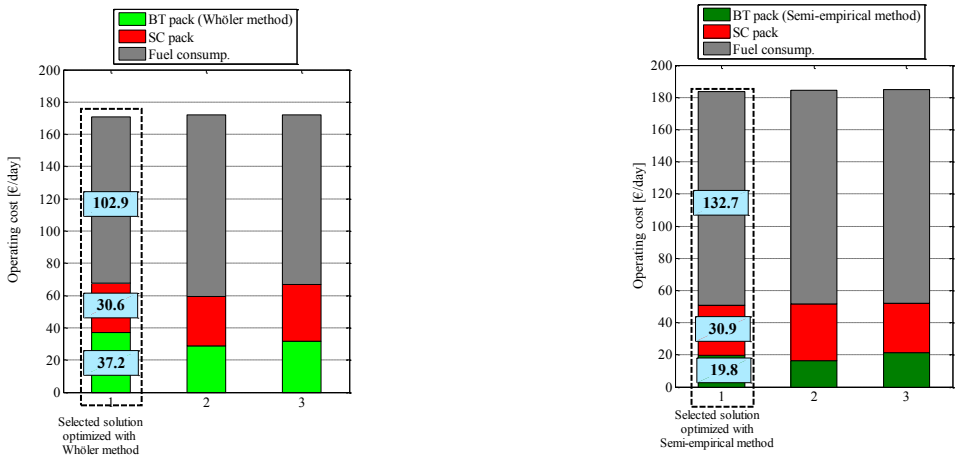

(a) Wöhler based optimization

(b) Semi-empirical based optimization

Fig. 6. Optimization results.

Comparing the optimisation results obtained for the two different lifetime models, it can be observed that in the case in which the Semi-empirical lifetime model was employed the optimisation tended towards a smaller battery sizing. In order to further explore the reasons behind such differences on the optimal case

selection, the lifetime of different battery and supercapacitor sizing solutions was evaluated. The optimal set of constraints calculated for each selected optimal solution (one for each of the two lifetime models) was maintained, while varying only the sizing of the dual ESS. Thereby, Fig. 7 shows the variation on the battery lifetime estimation (for each of the two lifetime models) considering the operating conditions defined for each of the two selected optimal solutions. The obtained lifetime values were scaled in p.u. basis considering as reference value the lifetime estimated with the Wöhler curve based lifetime model (the solution with the greatest lifetime in the leftmost plot in Fig. 7 is 1 p.u.). Results in Fig. 6 and Fig. 7 reveal a significant influence of the selected lifetime model on the selection of the optimal solution. Indeed, the semi-empirical lifetime model provided significantly larger lifetime estimations, which allowed the optimisation to increase the operation constraints while maintaining a smaller dual ESS sizing compared to the optimal case calculated with the Wöhler curve based lifetime model.

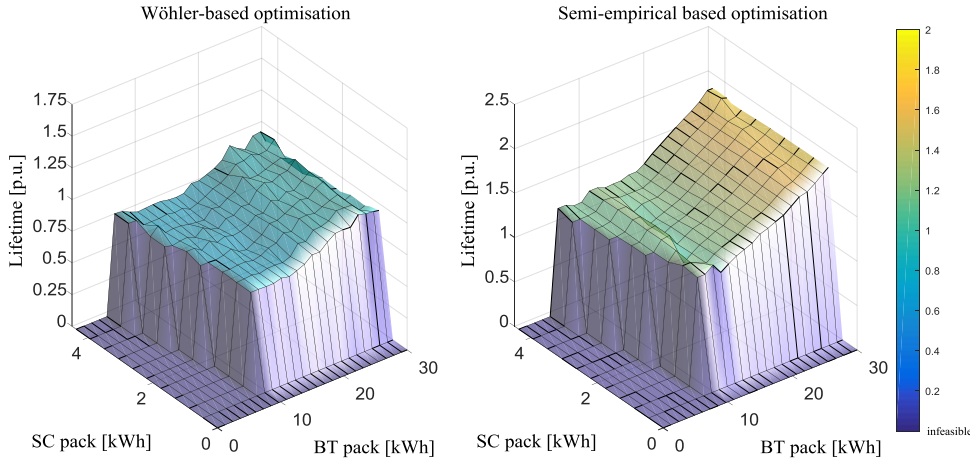

Fig. 7. Lifetime estimated for different battery and supercapacitor sizing values with the set of optimal operation constraints obtained with each of the two lifetime models considered. The lifetime is scaled in p.u. considering the maximum lifetime obtained for the Wöhler-based optimization.

As it can be observed in Fig. 8, in the optimal solutions considered for each of the considered lifetime models, the batteries are subjected to a repetitive SOC pattern, in which deep BT charge and discharges dominate its degradation. In Fig. 8(b) it can be observed that, the set of design variables assigned in the case of the optimisation performed with the semi-empirical model implies a better exploitation of the batteries, even accounting with a smaller dual ESS sizing. On the contrary, in the case of the optimisation performed with the Wöhler curve based model, the optimal set of operation constraints forces the battery to operate on a saturated status, in which the battery remains most of the time at low SoC levels, performing several micro-cycles in that region. The typical shape of Wöhler curves provides a large amount of cycles at low DoD ranges, driving the optimisation to that zone of battery operation. However, experimental battery ageing labours at low DoD values are costly and time consuming, and thus the reliability of any lifetime model in such area is usually lower.

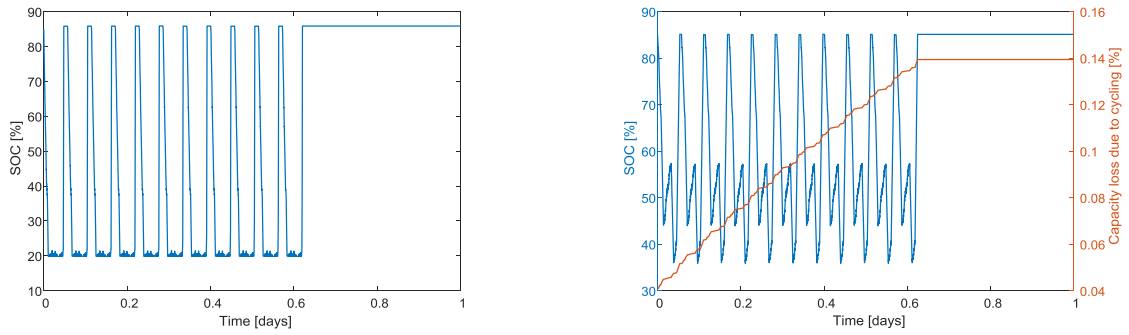

Fig. 8. Comparison of the daily battery operation profile for the optimal solutions calculated: (a) with the Wöhler curve based and (b) with the semi-empirical lifetime models.

On the contrary, the used semi-empirical lifetime model was validated under several operating conditions, including micro-cycles [5]. Thus, the lifetime estimations obtained in the low DoD operation area are more accurate than those obtained with the Wöhler curve based lifetime model, and the optimisation was driven to other areas of battery operation, in which an extended battery lifetime was achieved.

From the figures presented in this section, a significant impact of the lifetime model could be observed in the obtained optimisation results.

7 Conclusions

In this paper a thorough analysis of the influence of the battery lifetime model upon the optimisation results for ESS sizing and operation constraints was presented, considering a SHEB as the case study.

The obtained results suggest a significant influence of the lifetime model accuracy over the costs associated with both the operation of the hybrid bus and the sizing of the BT and SC. A difference of up to *c.a.* 8% on SHEB daily operation costs was estimated, depending on the employed lifetime model (170 €/day for the Wöhler based optimisation and 183 €/day for the semi-empirical model based optimisation). Similarly, if only dual ESS costs are considered, a difference of *c.a.* 25% was estimated depending on the employed lifetime model (67.8 €/day for the Wöhler based optimisation and 50.7 €/day for the semi-empirical model based optimisation).

The investigation of the influence of the supercapacitor lifetime model is foreseen as a future research line, as their lifespan would also depend on the operating conditions, but their ageing performance was simplified in the present study as it is also done in most publications in the literature.

References

[1] X. Hu, L. Johannesson, N. Murgovski, and B. Egardt, "Longevity-conscious dimensioning and power management of the hybrid energy storage system in a fuel cell hybrid electric bus," *Appl. Energy*, vol. 137, pp. 913–924, 2015.

[2] X. Luo, J. Wang, M. Dooner, and J. Clarke, "Overview of current development in electrical energy storage technologies and the application potential in power system operation," *Appl. Energy*, vol. 137, pp. 511–536, Jan. 2015.

[3] Z. Dimitrova and F. Maréchal, "Techno?economic design of hybrid electric vehicles and possibilities of the multi-objective optimization structure," *Appl. Energy*, vol. 161, pp. 746–759, Jan. 2016.

[4] G. Fuchs, B. Lunz, M. Leuthold, and D. U. Sauer, "Technology overview on electricity storage," *ISEA, Aachen, Juni*, 2012.

[5] E. Sarasketa-Zabala, E. Martinez-Laserna, M. Berecibar, I. Gandiaga, L. M. Rodriguez-Martinez, and I. Villarreal, "Realistic lifetime prediction approach for Li-ion batteries," *Appl. Energy*, vol. 162, 2016.

[6] V. I. Herrera, A. Saez-de-Ibarra, A. Milo, H. Gaztañaga, and H. Camblong, "Optimal energy management of a hybrid electric bus with a battery-supercapacitor storage system using genetic algorithm," *2015 International Conference on Electrical Systems for Aircraft, Railway, Ship Propulsion and Road Vehicles (ESARS)*. pp. 1–6, 2015.

[7] Z. Song, J. Li, X. Han, L. Xu, L. Lu, M. Ouyang, and H. Hofmann, "Multi-objective optimization of a semi-active battery/supercapacitor energy storage system for electric vehicles," *Appl. Energy*, vol. 135, pp. 212–224, Dec. 2014.

[8] E. Sarasketa-Zabala, I. Gandiaga, E. Martinez-Laserna, L. M. Rodriguez-Martinez, and I. Villarreal, "Cycle ageing analysis of a LiFePO4/graphite cell with dynamic model validations: Towards realistic lifetime predictions," *J. Power Sources*, vol. 275, pp. 573–587, Oct. 2014.

[9] V. Herrera, A. Milo, H. Gaztañaga, I. Etxeberria-Otadui, I. Villarreal, and H. Camblong, "Adaptive energy management strategy and optimal sizing applied on a battery-supercapacitor based tramway," *Appl. Energy*, vol. 169, pp. 831–845, 2016.

[10] W. A. Facinelli, *Modeling and Simulation of Lead-acid Batteries for Photovoltaic Systems*. University Microfilms, 1983.

[11] D. U. Sauer and H. Wenzl, "Comparison of different approaches for lifetime prediction of electrochemical systems—Using lead-acid batteries as example," *J. Power Sources*, vol. 176, no. 2, pp. 534–546, Feb. 2008.

[12] E. Sarasketa-Zabala, "A novel approach for Li-ion battery selection and lifetime prediction," Ik4-Ikerlan, 2014.

[13] E. Sarasketa-Zabala, I. Gandiaga, L. M. Rodriguez-Martinez, and I. Villarreal, "Calendar ageing analysis of a LiFePO4/graphite cell with dynamic model validations: Towards realistic lifetime predictions," *J. Power Sources*, vol. 272, pp. 45–57, Dec. 2014.

[14] V. I. Herrera, A. Milo, H. Gaztanaga, and H. Camblong, "Multi-Objective Optimization of Energy Management and Sizing for a Hybrid Bus with Dual Energy Storage System," *2016 IEEE Vehicle Power and Propulsion Conference (VPPC)*. pp. 1–6, 2016.

[15] Mathworks, "Fuzzy Logic Toolbox Use 's Guide R2017a," 2017.

Authors

Egoitz Martinez Laserna was born in 1989 in Vitoria-Gasteiz. He received his M.Sc in Electronic Engineering from the University of Mondragon, Spain, in 2013. He joined the Energy Business Unit of IK4-IKERLAN Technological Research Centre, Spain, in 2013. Currently he is pursuing a Ph.D. degree in IK4-IKERLAN focused on 2nd life battery performance, sizing and integration. His research interests include electrochemical energy storage systems, electric vehicles, renewable energy and energy management.

Victor Herrera Pérez received his Eng. degree in Electronic in 2012 with a specialization in Automatic Control and Industrial Networks from the Polytechnic School of Chimborazo (Ecuador). Since 2014 he is pursuing a Ph.D. degree in IK4-IKERLAN Technological Research Centre in Mondragón (Spain) as part of the EMVEM project from the ITN Marie Curie. His research is focused on the development of optimal energy management strategies for hybrid storage systems applied in vehicles and machines. His interests include new energy storage technologies, hybrid and electric vehicles and energy management.

Iñigo Gandiaga received a Diploma in Physics from the University of the Basque Country, UPV-EHU (Spain) in 2010. Energy Business Unit of IK4 Ikerlan Technology Research Centre in 2010. His research interests include different electrochemical energy storage technologies (EDLC, Li-ion and NiMH), particularly the lifetime and sizing of batteries for transport and stationary applications. He joined the Energy Business Unit of IK4-IKERLAN Technology Research Centre in 2010. His research interests include from the lifetime estimation and sizing studies of different electrochemical energy storage technologies (EDLC, Li-ion and NiMH) for heavy duty transport and stationary applications, to SOC/SOH estimation algorithms for lithium-ion Battery Management Systems.

Aitor Milo received the B.Sc. degree in electronics from the University of Mondragon, Spain, in 1993, the M.Sc. degree from the National Polytechnic Institute of Grenoble, Grenoble, France, in 1995, and the Ph.D. degree from the University of Mondragon, Spain, in 2011. He joined the IK4-IKERLAN Technology Research Centre in 1995 where he is currently working as a Researcher. His research interests include energy management strategies and optimization for hybrid systems and electricity distribution grid, vertical transport systems and electric transport with presence of renewable energy and storage systems.

Elixabet Sarasketa Zabala received her M. Sc. degree in Chemical Engineering from the Faculty of Engineering of Bilbao (ETSI de Bilbao, Spain) and Master in Energy Systems from the University of Gävle (HIG, Sweden) in 2009, and Ph. D in Engineering with International mention from Mondragon University (Spain) in 2014. She has been working at the Energy Business Unit of IK4-Ikerlan since 2009. She is currently focused on the development of energy storage solutions towards the competitiveness increase of different industrial customers focused on electric mobility and stationary applications. Her research interests and technical activities include reliability, safety and lifetime assessment of Li-ion battery technologies and advanced characterisation of batteries and EDLC. Her activities also include project management and group coordination, and was e.g. CTO of Batteries2020 EC project. She is also actively involved in dissemination activities, being co-author of various scientific publications and international conference speaker.

Haizea Gaztañaga received the B.Sc. degree in electronics from the University of Mondragon, Spain, in 2001 and the M.Sc. and Ph.D. degrees from the National Polytechnic Institute of Grenoble, Grenoble, France, in 2003 and 2006, respectively. In 2006 she joined the Control Engineering and Power Electronics Department of IK4-IKERLAN where she has participated in several industrial and research projects both as a researcher as well as a project manager. She is currently the project coordinator of the research activity of IK4-IKERLAN in the field of Electrical and Power Electronics Systems. Her main technical activities and interests include the design and control of power conversion systems for applications such as Renewable Energies, Transportation and Storage.